Metal Artifact Reduction in CT-Based Attenuation Correction of PET Data Using the Virtual Sinogram Concept

Mehrsima Abdoli, Mohammad Reza Ay, Alireza Ahmadian
Dept. Medical Physics and Biomedical Engineering & Research Center for Science and Technology in Medicine & Research Institute for Nuclear Medicine, Tehran University of Medical Sciences, Tehran, Iran
mabdoli@razi.tums.ac.ir, mohammadreza_ay@tums.ac.ir, ahmadian@sina.tums.ac.ir

Habib Zaidi
Division of Nuclear Medicine
Geneva University Hospital
Geneva, Switzerland
habib.zaidi@hcuge.ch

***Abstract* — The presence of high density materials in CT imaging is known to generate strong streak artifacts in CT images. This will obviously impact the generated μmaps, and as such could affect the reconstructed PET image during the CT-based attenuation correction (CTAC) procedure. Thus the attenuation maps (μmaps) generated from these images will likely propagate the artifacts to the resulting PET images. The main problem associated with current sinogram-based methods for metal artifact reduction is the difficulty in manipulating raw CT data which usually consist of large files saved in vendor's proprietary formats. The proposed method directly computes a virtual sinogram through forward projection of CT images to overcome the above mentioned cumbersome inconvenience. The metallic objects in the CT image are first segmented. This is followed by forward projecting the obtained metal-only image. Then, missing projection data affected by metallic objects are detected and replaced by interpolated values from neighboring data using the spline interpolation functions. The algorithm is applied to a polyethylene phantom scanned before and after insertion of metallic objects. The corrected and non-corrected μmaps are compared to artifact-free μmap. It was shown that the mean relative error in regions close to metallic objects is reduced by 30% after applying our method. In another experiment a Jaszczak phantom is used to evaluate the results of the algorithm on reconstructed PET images. The activity concentration error produced in PET images is reduced by 85%. Moreover, the reconstruction of attenuation correction factors shows an obvious reduction of metal artifacts in the generated μmaps after applying the proposed algorithm. This study reports results obtained from a limited set of experimental measurements, further evaluation using clinical data sets is ongoing.**

Keywords- PET/CT; Attenuation Correction; Metal Artifact; Quantification; Spline Interpolation; Virtual Sinogram

I. INTRODUCTION

In recent years, positron emission tomography (PET) has become an effective method for clinical diagnosis and assessment of response to therapy in oncology. To accurately measure the activity concentration in different tissues of the body, attenuation correction (AC) of PET images is mandatory. One of the most widely used techniques for AC on combined PET/CT systems consists in using computed tomography (CT) images, owing to the fact that CT images contain information about attenuation properties of biological tissues. The advent of in-line PET/CT scanners further stimulated the clinical use of CTAC in addition to using CT images for anatomical mapping and localization of the abnormalities visible on PET images.

However, the presence of high density metallic objects, such as dental fillings and hip prostheses, causes insufficient number of photons to reach the detectors. This results in the production of streak artifacts in CT images. These artifacts will likely propagate into PET images during the CT-based attenuation correction (CTAC) procedure and might deteriorate PET image quality and bias the quantitative analysis of radiopharmaceutical uptake. Therefore, before applying the CTAC procedure, metal artifacts must necessarily be removed.

Several techniques have been proposed for metal artifact reduction (MAR). In general, these methods can be categorized in two groups namely sinogram based and image based methods. In the first group, the correction is implemented on acquired sinogram space. Linear interpolation of the missing data is one of these methods [1]. Since the difference between metallic objects and other tissues' CT numbers is considerable, a simple thresholding can be used for segmenting the metallic objects. The extracted image is forward projected to determine the projections in the sinogram space which are affected by metallic objects. These projections are then replaced by linear interpolation of other projections in the same projection angle. Finally, the corrected image is obtained from the reconstruction of the corrected sinogram through inverse Radon transform. Cubic interpolation of unaffected projections is another way of replacing the missing projections [2].

Replacing missing projections by their unaffected correspondence is another method of this category [3]. In this method, instead of using an interpolation algorithm, missing projections are replaced by their corresponding unaffected projection, i.e. the opposite angular position in spiral scanning and the same angular position of the next slice in step scanning.

The second group of metal artifact reduction methods is based on image rather than the sinogram. Iterative deblurring [4], knowledge based [5] and segmentation [6] techniques are some examples of image-based methods. These methods are obviously less accurate than those used in the first group,

This work was supported by Tehran University of Medical Sciences and Research Center for Science and Technology in Medicine. HZ acknowledges the support of the Swiss National Science Foundation under grant No. 3152A0-102143.

978-1-4244-2902-8/09/$25.00 ©2009 IEEE

because detecting artifactual regions in the image precisely is nearly impossible.

It should be noted that metal artifact reduction techniques operating in the sinogram space are usually applied to raw projection data consisting huge encrypted files which can not be easily manipulated without extensive technical support from the vendors. In a previous study, we proposed to use a virtual sinogram instead of the acquired one, which is produced by forward projection of reconstructed CT images in Dicom format, to circumvent the above mentioned difficulties and make the correction procedure scanner independent [7]. The aim of this study is to investigate the potential benefits of the virtual sinogram based MAR method in a clinical environment using experimental phantom studies on a clinical PET/CT scanner. It should be emphasized that our goal is not to generate metal artifact free CT images appropriate for clinical diagnosis. Rather our MAR method aims at providing an artifact free μmap allowing to improve the accuracy of PET image quantification.

II. Materials and Methods

A. Phantoms and Scanning Protocols

To assess the impact of metal artifacts on different body tissues during the CTAC procedure, a 25 cm diameter cylindrical polyethylene phantom was used. This consists of 16 syringes (20 mm diameter), filled with different concentrations of K_2HPO_4 solution simulating attenuation properties of different tissues of the human body, ranging form soft tissue to bone. In order to generate metal artifacts in CT images, 4 metallic inserts were placed in the middle of the phantom. A clinical 64-slice CT scanner, the GE LightSpeed VCT (General Electric Healthcare Technologies, Waukesha, WI), was used to acquire images of the phantom. The phantom was scanned at 120 kVp and 200 mAs twice in the same position, with and without metal inserts. The scan without metallic inserts was performed to obtain an artifact free image that can serve as a reference image, allowing assessment of the accuracy of the MAR algorithm. This phantom was used to evaluate the μmaps generated from corrected CT images.

The second phantom used to evaluate the algorithm on reconstructed PET images is the so called Jaszczak phantom (Fig. 1). To assess the accuracy of the proposed MAR method on PET activity concentration quantification, the phantom was filled with 16.67 kBq/cc of ^{18}F. Four metallic inserts were placed inside the phantom to produce metal artifacts (see arrows in Fig. 1). This phantom was scanned on the Biograph 64-slice PET/CT scanner (Siemens Medical Solutions, Erlangen, Germany) at 120 kVp and 160 mAs where the PET emission data was acquired during 40 minutes. The images were reconstructed using the attenuation weighted ordered subsets – expectation maximization (AW-OSEM) iterative reconstruction technique.

B. ACF Reconstruction

For further evaluation of the proposed MAR algorithm, the attenuation maps of the phantom images, generated by the scanner, were evaluated. Given that the generated attenuation maps are not available to the user on the acquisition console, the generated attenuation correction factors (ACFs) were reconstructed. A MATLAB code was written to read the ACFs. The reconstruction procedure was performed using inverse Radon transform which requires knowledge of the exact specifications of the scanner. As the ACFs are generated along a parallel beam geometry, they were first converted to the fan beam geometry and then were backprojected to produce μmaps using a MATLAB code.

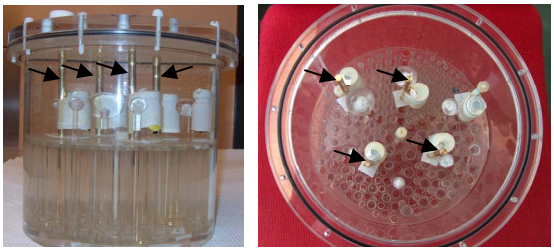

Figure 1. Photo of the Jaszczak phantom with 4 metallic inserts (arrows).

C. MAR Algorithm

Currently available sinogram-based MAR algorithms are based on the correction of raw data sinograms which are huge files that are not straightforward to manipulate. To simplify this approach, the proposed method uses the concept of virtual sinograms for implementation of MAR. A virtual sinogram is produced by fan beam forward projection of CT images in 2D, which is performed by a MATLAB routine. Reconstruction of the virtual sinogram through the inversion procedure might not result in diagnostic quality CT images for clinical use; however, it is suitable for the CTAC procedure owing to the low resolution of attenuation maps following downsampling and smoothing.

The first step of the algorithm consists in detecting the missing projection data in the sinogram, which are affected by metallic objects. The approach segments metallic objects by thresholding the original CT image thus allowing to obtain a metal-only image (Fig. 2b). This image is forward projected in 360 degrees to generate a sinogram reflecting information gathered for metallic objects, i.e. missed projections can be distinguished in this sinogram through their corresponding values. Zero values illustrate the non-affected projections and greater values determine the missed projections (Fig. 2d).

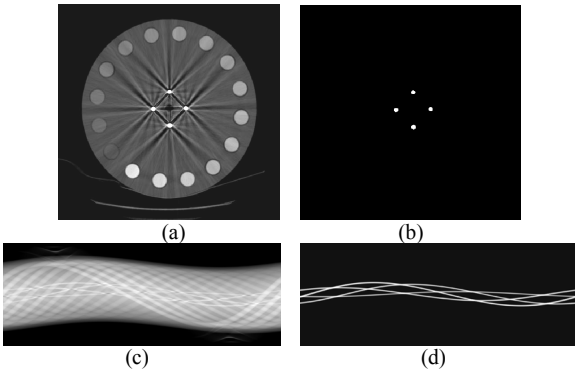

Figure 2. Detection of affected projections: (a) original CT image, (b) metal only image, (c) original sinogram and (d) metal-only sinogram.

The next step consists in replacing the missed projections in the virtual sinogram of the image by appropriate values. These values are obtained by interpolation of adjacent projections using the B-spline interpolation technique. Then the corrected sinogram is backward projected and an artifact free image is generated.

The corrected CT images are used to produce the μmaps in three stages. In the first stage, the corrected CT images are downsampled to be spatially matched to corresponding PET images. Next, the corrected CT images are smoothed to match the resolution of the PET scanner. This is achieved by applying a Gaussian filter with a proper kernel size to the CT images. The last step consists in mapping the linear attenuation coefficients from the low-energy x-rays to the corresponding PET energy (511 keV). This energy conversion is performed using a bilinear calibration curve.

To evaluate further the algorithm, the μmaps of the CT images of the polyethylene phantom without metallic inserts were also generated and compared to those derived from corrected images. This evaluation was performed by defining 26 regions of interest (ROIs) in different regions of the phantom. The ROI statistics of both corrected and artifact-free images were compared and the results summarized in the form of Box and Whisker plots.

Evaluation of the Jaszczak phantom was performed on reconstructed PET images. Knowing the exact activity concentrations within the phantom, activities of 50 ROIs in corrected PET images were compared to their true values. For statistical analysis a two-tailed paired t-test was used.

III. Results

Figures 3 and 6 show the performance results of the proposed MAR algorithm on CT images of the two phantoms containing metallic inserts. For the polyethylene phantom, the μmap was generated (Fig. 3b-c) whereas for the Jaszczak phantom, corrected CT images were used for CTAC of PET images (Fig. 6). The images obtained for the polyethylene phantom without metallic inserts in which no artifacts can be observed is illustrated in Fig. 3c. Regions corresponding to metallic inserts were replaced with values corresponding to metal in the artifact-free image for comparison with the corrected μmap.

As one can observe from Fig. 3d, the ROIs were defined in the polyethylene phantom on regions simulating different biological tissues (ROIs 1 to 16) and other regions containing metal artifacts (ROIs 17 to 26). The same ROIs were defined on the original μmap, corrected μmap and artifact-free μmap.

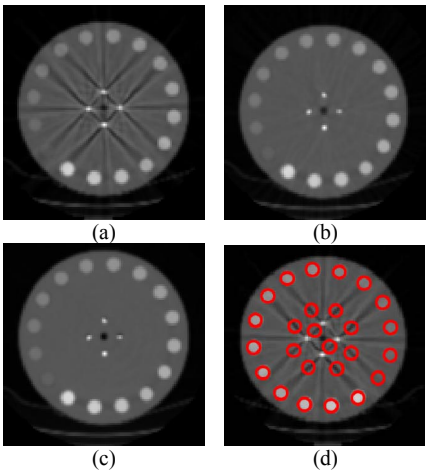

Figure 3. μmap obtained from (a) the original image, (b) the corrected image, (c) metal artifact-free image. (d) ROIs defined on the μmap to evaluate the accuracy of the metal artifact reduction technique.

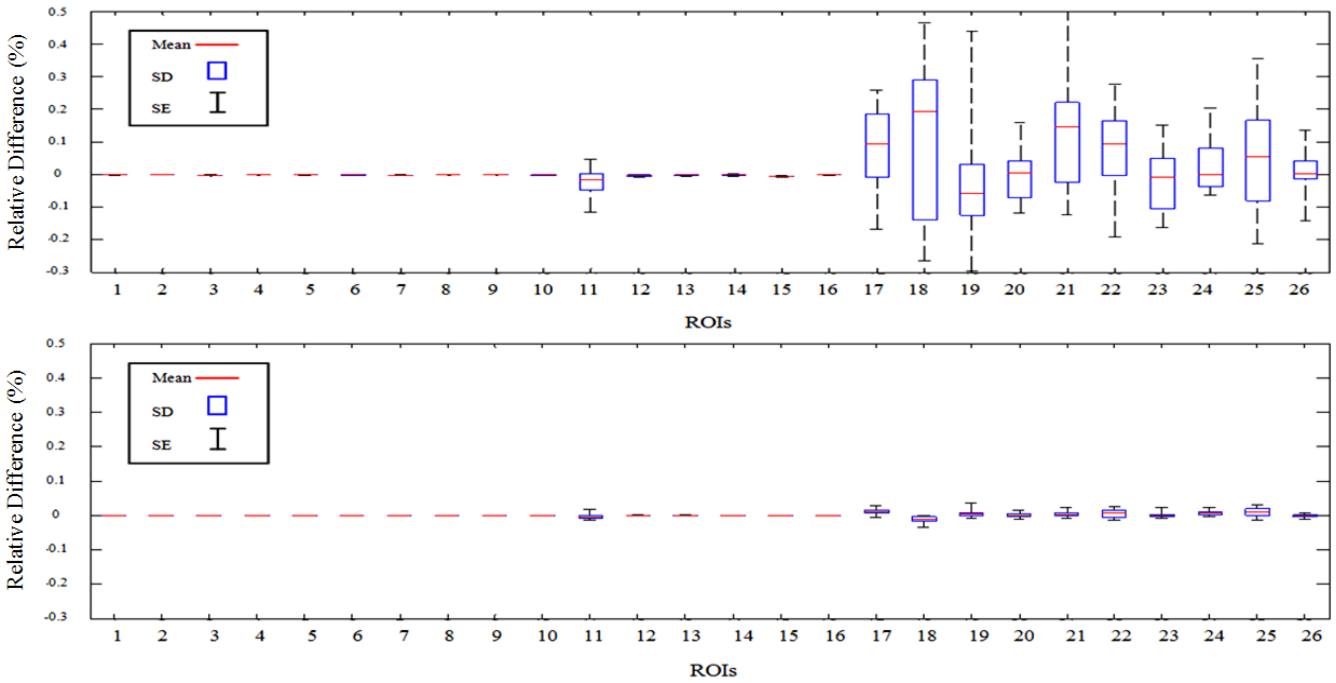

Figure 4. Box and Whisker plots showing relative differences for 26 ROIs between the original μmap and without-metal μmap (top) and the corrected μmap and without-metal μmap (bottom).

Thereafter the mean values, standard deviations and standard errors of these ROIs were reported in the Box and Whisker plots to illustrate the relative difference between the original μmap and the artifact-free μmap and that of the corrected μmap and the artifact-free μmap (Fig. 4).

Figure 5 shows the ACFs and μmaps obtained from reconstructions of ACFs corresponding to the original and corrected CT images of the Jaszczak phantom. It can clearly be seen that when using the proposed MAR algorithm, missed projections in the ACFs are replaced by appropriate values and as such, metal artifacts in the μmaps are considerably reduced. The reconstructed PET images of the Jaszczak phantom are illustrated in Fig. 6. Metal artifacts in non corrected μmap give rise to typical metallic objects related artifacts in the corresponding PET image (arrows in Fig. 6c).

Table 1 summarizes the statistical analysis results of the Jaszczak phantom. P-values are obtained from a two-tailed paired t-test statistical analysis. The mean value (in Bq/cc) and standard deviation of 50 ROIs in the corrected PET images of the phantom and the corresponding actual value are also given.

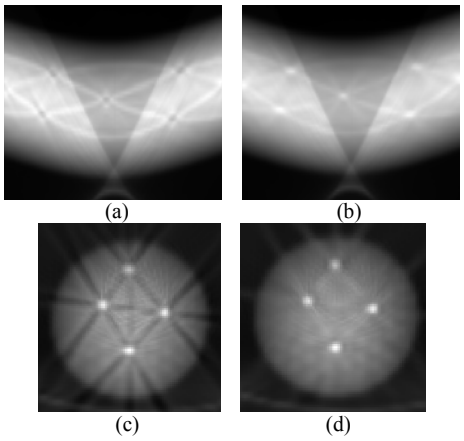

Figure 5. ACF sinograms generated by the PET/CT scanner using (a) non corrected CT image, (b) corrected CT image. (c) μmap before correction, (d) μmap obtained after MAR.

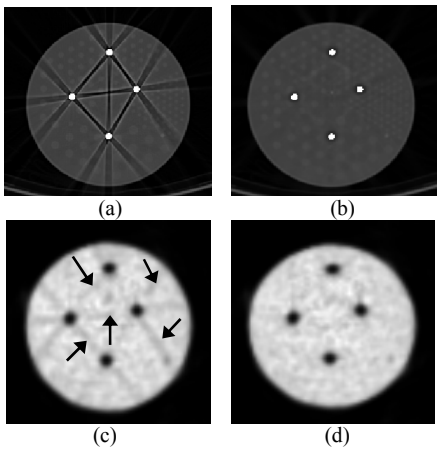

Figure 6. (a) Original CT image, (b) corrected CT image, (c) PET image without MAR (arrows show the artifacts generated through CTAC procedure), (d) PET image with MAR.

TABLE I. SUMMARY OF STATISTICAL ANALYSIS RESULTS OF PET IMAGES.

PET Image	Mean (kBq/cc)	SD	P-Value
Corrected PET image	16.54	0.64	0.0975
Uncorrected PET image	15.80	0.79	<0.0001
Actual activity concentration	16.67		

IV. DISCUSSION AND CONCLUSSION

The proposed MAR algorithm is suitable for generating metal artifact free μmaps in the presence of metallic objects that can be used for attenuation correction of PET data without the need to deal with the cumbersome task of reading raw CT data. The method is capable of reducing metal artifacts in regions adjacent to metallic objects.

As illustrated in Fig. 4 for the polyethylene phantom, metallic artifacts result in an immense difference between the original and the artifact free μmap especially in regions adjacent to metallic objects. It was also observed that following application of this MAR approach, the differences decrease considerably. In the original PET images of the Jaszczak phantom, an underestimation of activity concentration can be observed owing to the dark streaks caused by metallic objects. As a result, the mean value of the original image is less than the actual value. After applying the MAR algorithm, the mean value is very close to the actual value. In addition, the standard deviation of ROIs inside the phantom is reduced after application of the MAR algorithm. The statistical analysis did not reveal any statistically significant difference between the corrected and artifact-free images whereas ($p>0.05$) whereas statistically significant difference is obvious in the case of non-corrected PET images ($p<0.0001$).

It can be concluded that the proposed approach is fast and suitable for metal artifact reduction of CT images to be used in CTAC of corresponding PET data, especially for strong artifacts produced in regions adjacent to metallic objects. This method reduces the errors in the μmap from ~35% to ~5% and the errors in the corresponding PET data from ~6% to ~0.7%.

REFERENCES

[1] W. Kalender, R. Hebel, J. Ebersberger (1987) "Reduction of CT artifacts caused by metallic implants." Radiology 164:576-577.

[2] M. Bazalova, L. Beaulieu, S. Palefsky, F. Verhaegen (2007) "Correction of CT artifacts and its influence on Monte Carlo dose calculation." Med. Phys 34(6):2119-2132.

[3] M. Yazdi, L. Beaulieu (2006) "A novel approach for reducing metal artifacts due to metallic dental implants" IEEE Nucl. Sci. Symp. Conf. Rec. 4:2260-2263.

[4] G.Wang, D.L.Snyder, J. A.O'Sullivan, M.W.Vannier (1996) "Iterative Deblurring for CT Metal Artifact Reduction" IEEE Trans. Med. Imaging, 15(5):657-664.

[5] J.J.Hamill, R.C.Brunken, B.Bybel, F.P.DiFilippo, (2006) "A knowledge-based method for reducing attenuation artefacts caused by cardiac appliances in myocardial PET/CT" Phys. Med. Biol. 51:2901–2918.

[6] S. Mirzaei, M. Guerchaft, C. Bonnier, P. Knoll, M. Doat, P. Braeutigam (2005) "Use of segmented CT transmission map to avoid metal artifacts in PET images by a PET-CT device" BMC Nuclear Medicine, 5(3), 1-7.

[7] M. Abdoli, M.R. Ay, A. Ahmadian, N. Sahba, H. Zaidi (2008) "A novel approach for reducing dental filling artifacts in CT-based attenuation correction of PET data" European Congress for Medical and Biological Engineering , MBEC 2008, Belgium, IFMBE Proceedings 22, 492-495.